



Cite this: *Phys. Chem. Chem. Phys.*,  
2016, **18**, 11942

# The degree of $\pi$ electron delocalization and the formation of 3D-extensible sandwich structures†

Xiang Wang,<sup>a</sup> Qiang Wang,<sup>b</sup> Caixia Yuan,<sup>a</sup> Xue-Feng Zhao,<sup>a</sup> Jia-Jia Li,<sup>a</sup> Debao Li,<sup>b</sup> Yan-Bo Wu\*<sup>a</sup> and Xiaotai Wang<sup>c</sup>

DFT B3LYP/6-31G(d) calculations were performed to examine the feasibility of graphene-like  $C_{42}H_{18}$  and starbenzene  $C_6(BeH)_6$  (SBz) polymers as ligands of 3D-extensible sandwich compounds (3D-ESCs) with uninterrupted sandwich arrays. The results revealed that sandwich compounds with three or more  $C_{42}H_{18}$  ligands were not feasible. The possible reason may be the localization of  $\pi$  electrons on certain  $C_6$  hexagons due to  $\pi$ -metal interactions, which makes the whole ligand lose its electronic structure basis (higher degree of  $\pi$  electron delocalization) to maintain the planar structure. For comparison, with the aid of benzene (Bz) molecules, the SBz polymers can be feasible ligands for designing 3D-ESCs because the C-Be interactions in individual SBz are largely ionic, which will deter the  $\pi$  electrons on one  $C_6$  ring from connecting to those on neighbouring  $C_6$  rings. This means that high degree of  $\pi$  electron delocalization is not necessary for maintaining the planarity of SBz polymers. Such a locally delocalized  $\pi$  electron structure is desirable for the ligands of 3D-ESCs. Remarkably, the formation of a sandwich compound with SBz is thermodynamically more favourable than that found for bis(Bz)chromium. The assembly of 3D-ESCs is largely exothermic, which will facilitate future experimental synthesis. The different variation trends on the HOMO-LUMO gaps in different directions (relative to the sandwich axes) suggest that they can be developed to form directional conductors or semiconductors, which may be useful in the production of electronic devices.

Received 30th November 2015,  
Accepted 8th March 2016

DOI: 10.1039/c5cp07372c

www.rsc.org/pccp

## 1. Introduction

The discovery of sandwich structures of prototypical bis(cyclopentadienyl)iron and bis(benzene)chromium in the 1950s opened the door to modern organometallic chemistry.<sup>1</sup> The unprecedented geometries, novel  $\pi$ -metal multicenter bonding and widespread applications, such as molecular catalysis, electronics and pharmacology, have intrigued chemists for more than sixty years.<sup>2</sup> During this period, considerable attentions have been paid to the exploration of new types of sandwich structures. With careful elaboration, the metal centers have been extended from the traditional iron and chromium to other metal atoms and the outer ligands have been extended from traditional cyclopentadienyl (Cp) and benzene (Bz) to other monocyclic

aromatic hydrocarbons, anti-aromatic hydrocarbons, polycyclic aromatic hydrocarbons<sup>3</sup> and various inorganic compounds, including but not limited to the planar or cage-like boron hydride and the carboranes,<sup>4</sup>  $E_5^-$  ( $E = N, P, As, Sb, \text{ and } Bi$ ) compounds<sup>5</sup> and interestingly, planar hypercoordinate carbon (phC) species.<sup>6</sup> Very recently, an all metal sandwich structure  $Sb_6Au_3^{3-}$  was successfully crystallized.<sup>7</sup>

In addition to altering the types of metal centers and ligands in classical double decker one metal sandwich compounds, chemists have also been interested in incorporating sandwich structures into large molecules. The most studied non-classical sandwich pattern is the multiple decker sandwich compounds or 1D sandwich nanowires with uninterrupted sandwich arrays. Experimentally, the signals of an octadecker vanadium-iron-Cp compound have been recorded using gas phase spectroscopy<sup>8</sup> and organotransition metal metallocarboranes with pentadecker and hexadecker sandwiches have been crystallized.<sup>9</sup> Computationally, the infinite 1D sandwich chains (*i.e.* the 1D sandwich nanowires) have been elaborately designed and extensively characterized.<sup>10</sup>

Another non-classical sandwich pattern is the double decker sandwich structure bearing large polycyclic aromatic hydrocarbon as the ligands of multiple sandwiched metal centers. Philpott *et al.* employed zigzag-edged polycyclic aromatic hydrocarbons,

<sup>a</sup> Key Laboratory of Energy Conversion and Storage of Shanxi Province, Institute of Molecular Science, Shanxi University, Taiyuan, Shanxi, 030006, People's Republic of China. E-mail: wyb@sxu.edu.cn

<sup>b</sup> State Key Laboratory of Coal Conversion, Institute of Coal Chemistry, The Chinese Academy of Sciences, Taiyuan, Shanxi, 030001, People's Republic of China

<sup>c</sup> Department of Chemistry, University of Colorado Denver, Campus Box 194, P.O. Box 173364, Denver, Colorado 80217-3364, USA

† Electronic supplementary information (ESI) available: The table comparing the  $\omega$ B97X-D/6-31G(d) and B3LYP/6-31G(d) results and the figures with full sets of AdNDP results. See DOI: 10.1039/c5cp07372c

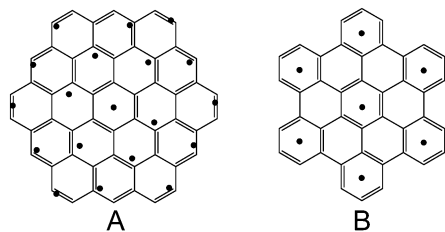


Fig. 1 Top view of the locations (black dots) of metal atoms in the double-decker sandwich compounds ( $(C_{54}H_{18})_2Pd_{19}$  (A) and  $(C_{42}H_{18})_2Cr_7$  (B)).

including  $C_{16}H_{10}$ ,  $C_{18}H_{12}$ ,  $C_{24}H_{12}$ ,  $C_{32}H_{14}$ ,  $C_{40}H_{16}$ ,  $C_{42}H_{16}$ , and  $C_{54}H_{18}$ , as the ligands of 4, 4, 7, 10, 13, 14, and 19 palladium atoms, respectively (see Fig. 1A for an example of  $(C_{54}H_{18})_2Pd_{19}$ )<sup>11</sup> and found that most of the palladium atoms were not located at the centers of the corresponding  $C_6$  rings because there are not enough  $\pi$  electrons to form the 18 electron shell structure around the metal centers. More reasonable examples of sandwich compounds were designed with armchair-edged polycyclic aromatic hydrocarbons, including  $C_{12}H_{10}$ ,  $C_{18}H_{12}$ ,  $C_{24}H_{14}$  and  $C_{42}H_{18}$ .<sup>12</sup> It can be noted that the number of  $C_6$  rings in these ligands is larger than those of sandwiched metals. As shown in Fig. 1B, the carefully selected sandwich sites enable the formation of an 18 electron shell structure around each of the chromium atoms.

Recently, a 3D-extensible sandwich framework was designed computationally by linking uninterrupted 1D sandwich chains with a hydrogen bond network.<sup>13</sup> However, to the best of our knowledge, if the chemical bonds are required for linking the uninterrupted multiple-decker sandwich compounds or 1D sandwich chains, the corresponding structure is unknown to date. 3D-extensible sandwich structures can also be seen as multiple-decker sandwich compounds or 3D-extensible crystals with 2D extensible ligands. In this sense, the ligands, which are most easily thought of, are polycyclic aromatic hydrocarbons and graphene. However, calculations have suggested that they are not feasible ligands because their  $\pi$  electrons delocalize to a greater degree than what 3D-extensible compounds need. In the following manuscript, taking  $C_{42}H_{18}$  as an example, we will explain why the graphene-like polycyclic aromatic hydrocarbons cannot be utilized as the ligands of multiple-decker sandwich compounds. Then, we will propose the feasible examples of 3D-extensible sandwich compounds (3D-ESC) on the basis of our previously reported  $C_6(BeH)_6$  polymers,<sup>14</sup> which have locally delocalized  $\pi$  electrons.

## 2. Computational methods

The geometries of the sandwich compounds were optimized with the B3LYP functional. The unscaled harmonic vibration frequencies were analysed at the same level to characterize the nature of the stationary points and evaluate the zero-point energy (ZPE) corrections. Since many of the sandwich compounds considered are very large in size, we need to use the basis set as small as possible. In this study, three basis sets, *i.e.* 6-311G(d,p) (BS1),

Table 1 Basis set calibration results on the binding energies (in kcal mol<sup>-1</sup>, relative to the free ligands and chromium). The experimentally measured binding energy for  $(Bz)_2Cr$  is 58.3 kcal mol<sup>-1</sup> (see ref. 3a)

	BS1	BS2	BS3
$(Bz)_2Cr$	-60.2	-79	-13.2
$(SBz)_2Cr$	-64.0	-84.1	-16.0
$(Bz)Cr(SBz)$	-78.2	-97.9	-30.2

6-31G(d) (BS2), and 6-31G(d) for C, H, and Be and LANL2DZ for Cr (BS3), were tested for the small sandwich structures and they were found to predict reasonable geometries. However, as shown in Table 1, they predict much different binding energies: BS1 gave very close binding energies to the experimental data, BS2 predicted reasonably and systematically larger binding energies, while BS3 predicted binding energies that are unacceptably smaller than the experimental data. Therefore, the BS1 results were used for calibration, the BS2 results are discussed in the text, while BS3 were disregarded. To prove that the predicted structures are not an artefact of the B3LYP functional, some selected small molecules were restudied at the  $\omega$ B97X-D/6-31G(d) level, which give similar results to those found at the B3LYP/6-31G(d) level. The  $\omega$ B97X-D/6-31G(d) and B3LYP/6-31G(d) results are compared in Table S1 (ESI<sup>†</sup>). As the designed sandwich complexes were not assembled by weak interactions, the basis set superposition error (BSSE) turned out to be insignificant<sup>‡</sup> and was not considered when the binding energies were computed. The adaptive natural density partitioning (AdNDP)<sup>15</sup> analyses were performed at the B3LYP/6-31G level using the AdNDP program and used to understand the chemical structure of the ligands and sandwich complexes. All calculations were performed using the Gaussian 09 package.<sup>16</sup>

## 3. Results and discussion

### 3.1. Planar structure and $\pi$ electrons localization

Appropriate planar 2D ligands are crucial for 3D-ESC. Since  $\pi$ -metal interactions are significant for the formation of a sandwich structure, the ligands should have the delocalized  $\pi$  electrons on the atoms that interact with metal center and it is also important that the delocalization of the  $\pi$  electrons is limited within these atoms. That is to say, the feasible ligands of a 3D-ESC should have locally delocalized  $\pi$  electrons. In this sense, graphene or graphene-like polycyclic aromatic hydrocarbons will not satisfy this requirement because the delocalization of the  $\pi$  electrons in polycyclic aromatic hydrocarbons is not limited to an individual ring. We employed the smallest species, *i.e.* planarized biphenyl, as an example to study the  $\pi$  electron structures. As shown in Fig. 2A, the AdNDP analyses revealed two six-center-two electron (6c-2e) and four four-center-two-electron

<sup>‡</sup> For the sandwich complexes studied in this study, the weakest bonding interaction is the formation of inter-units HBB from two free BeH groups with the binding energy ranging from 24.0 to 30.9 kcal mol<sup>-1</sup> at the B3LYP/6-31G(d) level (Table 3). As a demonstration, we calculated the BSSE for the formation of a HBB between two units of 2 to form 2PP<sub>2</sub>, which gives a negligible value of 2.3 kcal mol<sup>-1</sup>. Thus, there will not be an obvious difference if the BSSE are considered.

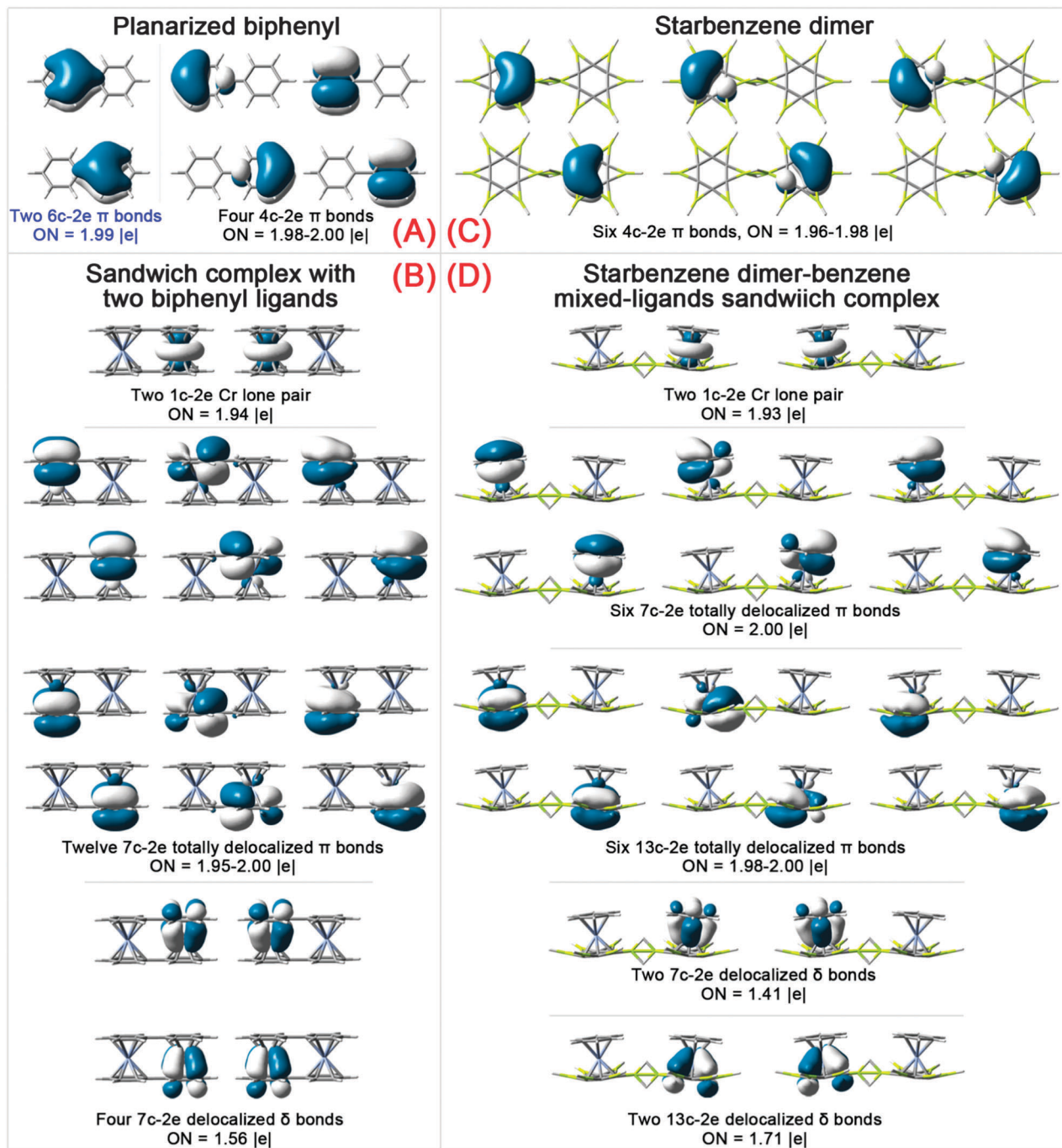


Fig. 2 An AdNDP view of the  $\pi$  electron structure on planarized biphenyl and the SBz dimer and that of the valence electron pair around the Cr atoms in selected sandwich complexes.

(4c-2e)  $\pi$  bonds. Though the 4c-2e bonds were located on one  $C_6$  ring, the 6c-2e bonds were delocalized on both  $C_6$  rings. In a previous study, the Boldyrev group analysed the  $\pi$  electron structure of graphene using the AdNDP approach and proposed that there are two  $\pi$  electrons located on each  $C_6$  hexagon, *i.e.* the  $\pi$  electrons are not fully delocalized.<sup>17</sup> However, such a degree of localization is not enough because more electrons are generally required for a  $C_6$  hexagon that caps the metal (in the case of Cr, six  $\pi$  electrons on each ligand are necessary) to form the

18 electron shell structure around it. The formation of a sandwich structure may further localize the  $\pi$  electrons, but such localization will destroy the basis of the electronic structure for maintaining the planar geometry of the ligands.

To prove the abovementioned analyses, we calculated the double-, triple- and quadruple-decker sandwich compounds bearing  $C_{42}H_{18}$  as the ligand. A previous study on the double-decker compound  $D_{6h}(C_{42}H_{18})_2Cr_7$  using the pure functional and plane wave basis set suggested the energy minimum nature.<sup>12</sup>

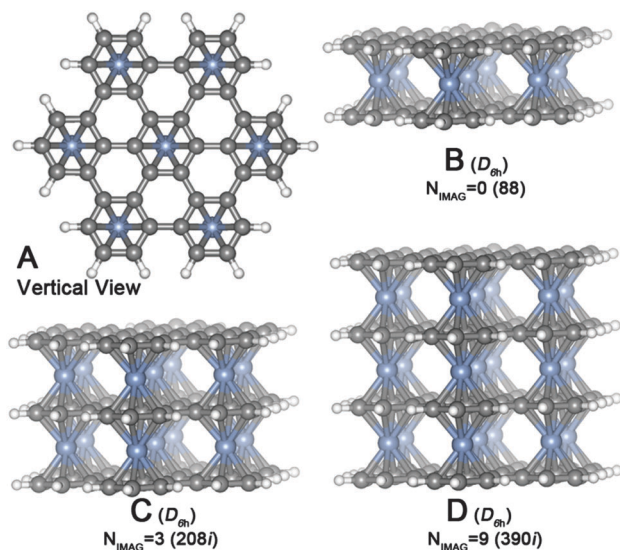


Fig. 3 The vertical view of the sandwich compound bearing graphene-like  $C_{42}H_{18}$  ligands (A) and the optimized structures, the number of imaginary frequencies ( $N_{\text{IMAG}}$ ) and lowest vibrational frequencies (in parenthesis after the  $N_{\text{IMAG}}$ ) of the double-, triple- and quadruple-decker sandwich compounds (B–D) at the B3LYP/BS2 level. Color codes: C: grey, H: white and Cr: cyan.

We recalculated this compound at a more reliable B3LYP/BS2 level and confirmed its energy minimum nature (the lowest vibrational frequency is  $88\text{ cm}^{-1}$ , see Fig. 3B). Nevertheless, when a triple decker sandwich structure is formed, all the  $\pi$  electrons on the middle decker ligand are thoroughly localized at the corresponding  $C_6$  hexagons and thus, this intermediate ligand may lose its basis in electron structure for maintaining the planarity. Consequently, as shown in Fig. 3C, the triple-decker sandwich compound bearing  $C_{42}H_{18}$  ligands is a third-order saddle point and the vectors of the imaginary frequencies (IFs) correspond to a break in the planar structures of the  $C_{42}H_{18}$  ligands. Similarly, the quadruple-decker sandwich compound (Fig. 3D) is a ninth-order saddle point with same type of IFs.

As shown in Fig. 2B, the AdNDP analysis of the small model sandwich complex bearing two biphenyl ligands suggest 9 orbitals about the d orbital of the Cr atom and  $\pi$ -d interactions in each sandwich unit, forming the stable 18 electron shell structure around the Cr atom. Remarkably, no orbital about the  $\pi$  orbitals of the biphenyl that was distributed on the two  $C_6$  rings can be found, which proved that the  $\pi$  electrons on biphenyl are localized when the sandwich arrangements were formed.

If we consider these sandwich compounds as fused sandwich chains, the  $C_6$  hexagons in the chains are linked together through direct C–C bonds, which establish the connection among the  $\pi$  electrons of individual  $C_6$  rings. We speculate that this may be the key reason why maintaining the planar structure of polycyclic aromatic hydrocarbons is in conflict with the formation of the 3D-ESC. According to this speculation, if the bonding among the  $C_6$  hexagons does not establish the connection among their  $\pi$  electrons, the corresponding ligand may be feasible for designing the 3D-ESC.

### 3.2. Examples of feasible ligands

To prove that the planarity of planar tetra-coordinate carbon (ptC)<sup>18</sup> can be used to construct flat, tubular and cage-like nanomolecules, which are shaped similar to graphene, carbon nanotubes and fullerene, we designed a series of monocyclic ptC-containing compounds  $D_{nh} C_n(\text{BeH})^q$  ( $n = 4-9$ , and  $q = 0, \pm 1, -2$ ), called starenes after their star-like geometries and aromatic nature. Previously, some species with star-like geometries have been reported.<sup>19</sup> The counterpart of benzene (Bz),  $D_{6h} C_6(\text{BeH})_6$ , called starbenzene (SBz), can be assembled into three shapes of flat, three shapes of tubular and one cage-shape nanomolecules *via* forming inter-SBz hydrogen bridge bonds (HBBs).<sup>14</sup> The HOMO–LUMO gaps of the polycyclic aromatic hydrocarbons reduce when they have more  $C_6$  rings. We found that assembling more SBz units into the polymer had no obvious influence on their HOMO–LUMO gap, which suggests that the formation of HBBs does not establish the connection among the  $\pi$  electrons of each SBz unit.

Our guess was proved by AdNDP analysis of the electron structures. As shown in Fig. 2C, the AdNDP results reveal that there are three four-center-two-electron (4c–2e)  $\pi$  orbitals on the  $C_6$  hexagon of each SBz unit. Our previous studies have also shown the large ionic character of C–Be bonding, which we attributed to be the main reason why the  $\pi$  electrons in one  $C_6$  ring do not connect to that of a neighbouring  $C_6$  ring.

### 3.3. Sandwich compounds with pure SBz ligands

Our previous study also showed that SBz has similar  $\pi$  orbitals to Bz, thus we wondered whether SBz can serve as the ligand of a sandwich compound. The answer turned out to be “yes”. For a convenient description, the bold Arabic numerals and its single and double quotation marked forms (*e.g.* 3, 3', and 3'') represent the eclipsed, staggered and neither eclipsed nor staggered structures of chain-like sandwich compounds, respectively. By replacing Bz in bis(Bz)chromium ((Bz)<sub>2</sub>Cr) with SBz, the classical shape of the sandwich compound bis(SBz)chromium ((SBz)<sub>2</sub>Cr) can be constructed. (Bz)<sub>2</sub>Cr (Fig. 4) turned out to have an eclipsed  $D_{6h}$  structure using both crystallography and gas phase spectroscopy,<sup>1c,3</sup> and this structure also had a minimum at the B3LYP/BS2 level. As a comparison, the eclipsed  $D_{6h}$  (SBz)<sub>2</sub>Cr (**1**) is a transition state (TS) with an IF at  $31i\text{ cm}^{-1}$ , whose vector is related to the counter-rotation of two aromatic ligands. The excurvate BeH groups and the longer C–Cr distance than that found in (Bz)<sub>2</sub>Cr (2.191 vs. 2.155 Å) revealed the non-negligible repulsion between the two SBz ligands. When the geometry was adjusted to the staggered form (**1'**, Fig. 4) to minimize this repulsion, the IF was eliminated. Nevertheless, **1'** is only 1.7 kcal mol<sup>−1</sup> lower in energy than **1** at the B3LYP/BS2 level, suggesting the high rotational freedom between the SBz ligands. Though the replacement of Bzs with SBzs will bring more repulsion, such replacement, as estimated by the reaction energy (RE), is exothermic by  $-4.8\text{ kcal mol}^{-1}$  (Table 2), revealing the stronger affinity between the SBz ligands and Cr than that found between the Bz ligands and Cr.

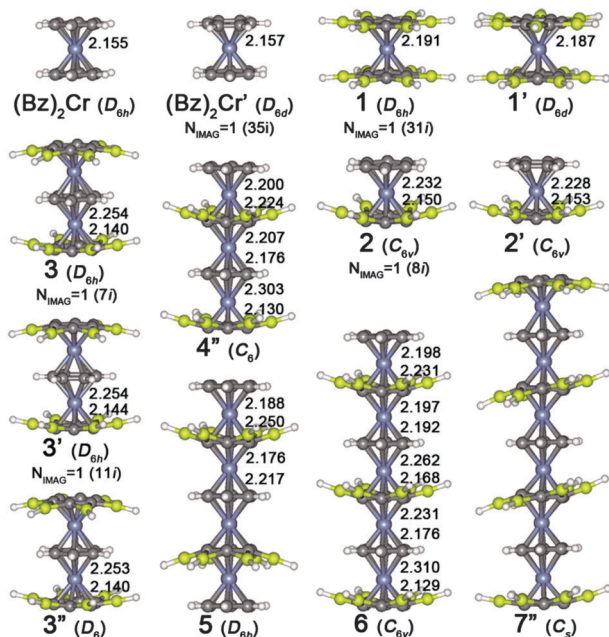


Fig. 4 The B3LYP/BS2 optimized structures of 1D sandwich chains. The necessary C–Cr bond lengths are given for the compounds with six-fold axis. The number of imaginary frequencies ( $N_{\text{IMAG}}$ ) and the lowest vibration frequencies (values in the parenthesis after the  $N_{\text{IMAG}}$ ) is given for the non-equilibrium structures. Color code: C: grey, H: white, Be: yellow, Cr: cyan.

We then tried to use the 2D polymer of SBz as the ligand in the sandwich structures. However, to form such a structure, the SBz polymers should be placed parallel to allow the  $C_6$  cores in one decker face those in the neighbour deckers. Such positioning makes it difficult to reduce the inter-deckers C–C distances to the required value of about 3.40 Å because the inter-decker H–H distances will be reduced to about 1.20 Å. Such short distance will generate the irresistible repulsion to destroy the sandwich structures.

Table 2 The point groups (PG), lowest vibrational frequencies ( $\nu_{\text{min}}$ , in  $\text{cm}^{-1}$ ), HOMO–LUMO gaps (Gap, in eV), total binding energy ( $\text{BE}_1$ , in  $\text{kcal mol}^{-1}$ ) relative to isolated Bz, SBz and Cr, reaction energies (RE, in  $\text{kcal mol}^{-1}$ ) for the replacement of Bz in  $(\text{Bz})_2\text{Cr}$  with SBz to form  $1'$  or  $2'$  and the binding energies for extending a decker of the 1D chains ( $\text{BE}_{1\text{D-ext}}$ , in  $\text{kcal mol}^{-1}$ ) of the 1D MDSCs at the B3LYP/BS1 level

	BS	PG	$\nu_{\text{min}}$	Gap	$\text{BE}_1$	RE	$\text{BE}_{1\text{D-ext}}$
$(\text{Bz})_2\text{Cr}$	BS1	$D_{6h}$	28	4.05	−60.2		
$1'$	BS1	$D_{6d}$	37	3.27	−64.0	−3.8	
$2'$	BS1	$C_{6v}$	15	3.80	−78.2	−18.0	
$3''$	BS1	$D_6$	9	3.61	−134.6		−56.6 <sup>a</sup>
$4''$	BS1	$C_6$	8	3.13	−183.4		−48.8 <sup>b</sup>
5	BS1	$D_{6h}$	14	2.75	−225.8		−42.4 <sup>b</sup>
6	BS1	$C_{6v}$	4	2.69	−285.7		−59.9 <sup>a</sup>
$(\text{Bz})_2\text{Cr}$	BS2	$D_{6h}$	39	4.06	−79.3		
$1'$	BS2	$D_{6d}$	37	3.24	−84.1	−4.8	
$2'$	BS2	$C_{6v}$	16	3.75	−97.9	−18.6	
$3''$	BS2	$D_6$	8	3.59	−172.0		−74.1 <sup>a</sup>
$4''$	BS2	$C_6$	5	3.12	−238.2		−66.3 <sup>b</sup>
5	BS2	$D_{6h}$	8	2.74	−298.1		−59.9 <sup>b</sup>
6	BS2	$C_s$	6	2.66	−375.5		−77.4 <sup>a</sup>

<sup>a</sup> Adding Cr and SBz. <sup>b</sup> Adding Cr and Bz.

### 3.4. Mixed-ligand sandwich compounds

To utilize the unique electron structure of the SBz polymers, the inter-decker distances should be augmented to avoid the steric repulsions among the bridged H atoms. This positioning leaves space, which can be filled by a special intermediate decker. Since the SBz polymer deckers can support strong enough sustainment, it is dispensable for the whole middle decker to be one molecule. Herein, Bz caught our eyes.  $(\text{Bz})_2\text{Cr}$  can adopt an eclipsed structure because the repulsion between the Bz ligands is small enough to be ignored. Therefore, if Bz can form mixed-ligand sandwich compounds with SBz, the former can be a reasonable middle decker. We studied this possibility by replacing a Bz ligand in  $(\text{Bz})_2\text{Cr}$  with SBz to form an eclipsed mixed-ligand sandwich compound  $(\text{Bz})\text{Cr}(\text{SBz})$  (2, see Fig. 4). At the B3LYP/BS2 level, 2 is a TS with an IF at  $8i \text{ cm}^{-1}$  and releasing the strain shown by the IF leads to the staggered energy minimum  $2'$  (Fig. 4). In  $2'$ , the C–Cr distances for SBz–Cr bonding is shorter than that found for Bz–Cr bonding (2.153 vs. 2.228 Å), which confirms the higher affinity of Cr to SBz than to Bz. The higher affinity can also be proved by the thermodynamics: the replacement of a Bz ligand in  $(\text{C}_6\text{H}_6)_2\text{Cr}$  with a SBz is exothermic by  $-18.6 \text{ kcal mol}^{-1}$  (see the REs in Table 2). When compared with  $-4.8 \text{ kcal mol}^{-1}$  for complete replacement of Bz with SBz, the mixed ligand sandwich compound possesses a superior thermodynamic priority than the pure ligand sandwich compounds  $(\text{C}_6\text{H}_6)_2\text{Cr}$  and  $1'$ , which can promote the generation of  $2'$  in the experiments rather than the mixture of  $(\text{Bz})_2\text{Cr}$ ,  $1'$  and  $2'$ .

The mixed-ligand sandwich structures are not limited in the double decker. By adding the Cr–Bz and Cr–SBz deckers, 1D multiple decker sandwich compounds (MDSCs) can be formed. We constructed such MDSCs with three to seven deckers for demonstration. As shown in Fig. 4, the triple- and quadruple-decker sandwich chains prefer neither the eclipsed nor the staggered structures ( $3''$  and  $4''$ , Fig. 4). The energy difference between these three shapes is less than  $0.8 \text{ kcal mol}^{-1}$ . Interestingly, the longer quintuple- and sextuple-decker complexes prefer the eclipsed structure (5 and 6, Fig. 4) and both their energies are  $1.7 \text{ kcal mol}^{-1}$  more stable in energy than their staggered isomers. Both the eclipsed and staggered septuple-decker sandwich complex (7 and  $7'$ ) are not the energy minima and the vectors of the imaginary frequencies tend to break the perfect six-fold axis, resulting in  $7''$  with a  $C_s$  geometry.

As shown in Fig. 4, for chains with more than two deckers, the C atoms in the SBzs at the terminal of the chains have the shortest C–Cr distance ( $\sim 2.14 \text{ Å}$ ), while that in the Bzs neighbouring, such SBz will have the longest C–Cr distance ( $\sim 2.30 \text{ Å}$ ). The other C–Cr distances for both SBzs and Bzs are almost identical. As estimated by the binding energies for extending a decker of the 1D chains ( $\text{BE}_{1\text{D-ext}}$ , Table 2) by adding a SBz–Cr decker to the sandwich chain, the binding energies are  $-74.1$  and  $-77.4 \text{ kcal mol}^{-1}$ , respectively, which are larger than those found when adding a Cr–Bz layer ( $-66.3$  and  $-59.9 \text{ kcal mol}^{-1}$ , respectively). The energetic results proved again the stronger affinity of SBz–Cr than that found for Bz–Cr.

The large total binding energies ( $BE_1$ ) indicate the good thermodynamic stability of the mixed-ligand 1D MDSCs.

### 3.5. Assembling the 3D-ESCs

The SBz units can be assembled into 2D-extensible planar sheets by forming inter-SBz HBBs. Can the mixed-ligand sandwich chains be assembled together by forming inter-SBz HBBs? In this study, 2', 3'' and 4''' were taken as examples to explore the possibility of forming 3D sandwich compounds. According to our calculation results, the formation of the HBBs can generate weak steric repulsions to let the SBz and Bz ligands in the unit chains to adopt the eclipsed arrangement in the assembled large molecules. Thus, we use 2, 3 and 4 to describe the unit chains for the convenient description. For the same purpose, the polymers reported in the following are named as "MLL<sub>n</sub>" (for example, 2PP<sub>7</sub>), where "M", "LL" and the subscript "n" denote the sandwich chain monomer (2), the linking pattern (PP) and the number of monomers (7 monomers), respectively. According to the different linking modes, three shapes of SBz polymers can be assembled. Correspondingly, using the same linking modes, three shapes of sandwich chain polymers can be assembled.

By forming the inter-chain HBBs in a point-to-point manner (PP, Fig. 5), the mixed-ligand MDSCs 2 and 3 can be assembled into the dimers, 2PP<sub>2</sub> ( $C_{2v}$ ) and 3PP<sub>2</sub> ( $D_2$ ) and trimers, 2PP<sub>3</sub> ( $C_{3v}$ ) and 3PP<sub>3</sub> ( $D_{3h}$ ), and they are the energy minima at the B3LYP/BS2 level. The average binding energies (BE) of HBB ( $BE_{HBB}$ , Table 3) for the double-decker polymers 2PP<sub>2</sub> and 2PP<sub>3</sub> are  $-29.0$  and  $-29.1$  kcal mol<sup>-1</sup>, respectively, which is slightly less than that found for the triple-decker polymers 3PP<sub>2</sub> and 3PP<sub>3</sub> ( $-30.9$  and  $-30.8$  kcal mol<sup>-1</sup>, respectively). We then constructed septamers, *i.e.* 2PP<sub>7</sub> ( $C_{6v}$ ) and 3PP<sub>7</sub> ( $D_{6h}$ ), to examine the extensibility. At the B3LYP/BS2 level, they are the energy minima and the  $E_{HBB}$  values are  $-28.8$  and  $-30.4$  kcal mol<sup>-1</sup>, respectively, which are very similar to that found for 2PP<sub>2</sub>/2PP<sub>3</sub> and 3PP<sub>2</sub>/3PP<sub>3</sub>.

Herein, we wondered whether the degree of electron delocalization in the SBz polymers was changed when the sandwich arrangements were formed. We performed AdNDP analysis on the smallest molecule 2PP<sub>2</sub> to understand its electronic structure. As shown in Fig. 2D, there are also 9 orbitals concerning the Cr atoms in each sandwich unit, forming the stable 18 electron shell structure around each Cr atom. Except for a  $d(z^2)$  orbital, the other eight orbitals have obvious  $\pi$ -d interaction character and the delocalization of the  $\pi$  electrons is restricted on each C<sub>6</sub>-Cr moiety. Therefore, in spite of the interactions with the d orbitals, there are no obvious differences in the degree of  $\pi$  electron delocalization before and after the formation of the sandwich arrangements.

In the PP shape polymers of the sandwich chains, they have the smallest strains because all the HBBs are arranged along the BeH directions. Alternatively, the sandwich chain monomers can be assembled in an edge-to-edge (EE) manner to give another shape of sandwich polymer. At the B3LYP/BS2 level, the EE-fused 2EE<sub>2</sub> ( $C_{2v}$ ) and 3EE<sub>2</sub> ( $D_{2h}$ ) are the energy minima (Table 3). As expected, the  $E_{HBB}$  values in double-decker 2EE<sub>2</sub> ( $-24.4$  kcal mol<sup>-1</sup>) and triple-decker 3EE<sub>2</sub> ( $-25.6$  kcal mol<sup>-1</sup>) are less than that of the corresponding PP-fused polymers and reflect the higher strain of EE fusion than PP fusion. Further extensibility

of EE fusion was checked by the studies of the hexamers. At the B3LYP/BS2 level, 2EE<sub>6</sub> ( $C_{6v}$ ) and 3EE<sub>6</sub> ( $D_{6h}$ ) (Fig. 5) are the energy minima with  $E_{HBB}$  values of  $-23.3$  and  $-24.7$  kcal mol<sup>-1</sup>, respectively, reducing slightly relative to that of 2EE<sub>2</sub> and 3EE<sub>2</sub> ( $-24.0$  and  $-25.6$  kcal mol<sup>-1</sup>) at the same level.

The combination of PP and EE fusions led to the PE shaped structures. The B3LYP/BS2-optimized structures of 2PE<sub>4</sub> and 3PE<sub>4</sub> are shown in Fig. 5. They are the energy minima with the lowest vibrational frequencies of 10 and 18 cm<sup>-1</sup>, respectively (Table 3). The  $E_{HBB}$  values of  $-25.3$  and  $-26.9$  kcal mol<sup>-1</sup> lie between the PP- and EE-assembled polymers.

The possibility of forming 3D sandwich polymers with more than three deckers was examined by studies on the representative species, PP-shape dimer/trimer, EE-shape dimer and PE-shape tetramer of 4. The optimized structures of 4PP<sub>2</sub> ( $C_2$ ), 4PP<sub>3</sub> ( $C_{3v}$ ), 4EE<sub>2</sub> ( $C_{2v}$ ) and 4PE<sub>4</sub> ( $C_{2v}$ ) are shown in Fig. 5. As shown in Table 3, they are energy minima on the PES at the B3LYP/BS2 level. The  $E_{HBB}$  values are  $-29.9$ ,  $-29.7$ ,  $-24.4$  and  $-25.8$  kcal mol<sup>-1</sup>, lying between the values of the corresponding shapes of double- and triple-decker sandwich polymers.

### 3.6. Understanding these sandwich compounds from a different perspective

In the abovementioned description, the 3D-ESCs were designed by fusing the 1D sandwich chains *via* the formation of HBBs. Alternatively, they can be seen as the consecutive accumulation of the SBz-polymer-chromium decker and Bz-chromium decker. Because the SBz polymers can retain the planarity with  $\pi$  electrons delocalized only on each C<sub>6</sub> hexagon, the planarity can be maintained when both sides of their C<sub>6</sub> hexagon interact with chromium. As shown in Fig. 5, for the double-decker sandwich compounds 2PP<sub>n</sub>, 2EE<sub>n</sub> and 2PE<sub>n</sub>, the SBz polymers are a little excurvate due to the small repulsion between the Bz ligands, while for the triple-decker sandwich compounds 3PP<sub>n</sub>, 3EE<sub>n</sub> and 3PE<sub>n</sub>, almost all the C<sub>6</sub> hexagons in each SBz polymer are co-planar. As tabulated in Table 3, the relatively large total BEs with regard to Bz ligands, Cr atoms and SBz polymer ligands ( $BE_2$ ) suggest the formation of 3D-ESCs on the basis of 2D SBz ligands is thermodynamically favourable. Remarkably, the middle decker, which consists of Bz ligands, separated the two SBz polymer deckers and the inter-atomic distances between H atoms in the HBBs of different deckers range from 4.252 Å to 4.619 Å. Such positioning eliminates the steric collisions discussed above. These sandwich compounds can be seen as the rudiment of 3D-ESCs. The binding energies for increasing the new SBz deckers ( $BE_{3D-ext}$  as tabulated in Table 3) are a little less than the  $BE_2$  of the double-decker sandwich frameworks. Nevertheless, the large  $BE_{3D-ext}$  values reveal the energetically favourable extending process. Although the larger 3D-ESCs are unaffordable for our current computational resources, we think the further extension of the structures should be feasible if the extending modes are not changed.

### 3.7. Variation of the HOMO-LUMO gaps

As shown in Table 3, when the number of the sandwich unit 2 (double-decker) and 3 (triple-decker) increases from two to

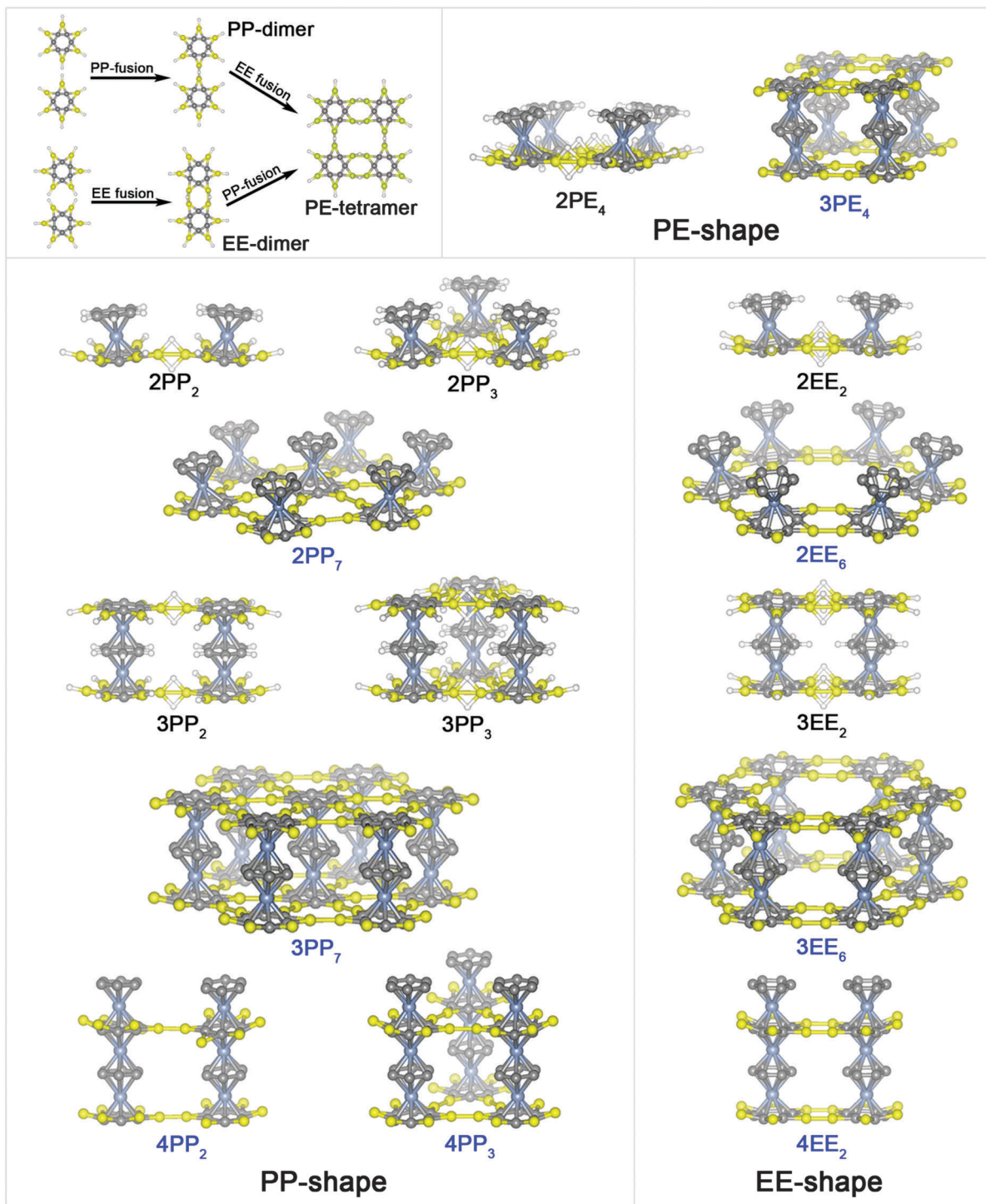


Fig. 5 Explanation of PP, EE and PE fusions and the B3LYP/BS2 optimized structures of 3D-extensible sandwich compounds. The H atoms in the large molecules (the molecules with blue names) are hidden for clarity.

seven, the HOMO–LUMO gaps of the PP-shape sandwich polymers only decrease from 3.68 and 3.64 eV to 3.30 and 3.31 eV, respectively. Similarly, when the number of the sandwich unit 2 and 3 increases from two to six, the HOMO–LUMO gaps of the EE-shape sandwich polymers only decrease from 3.62 and 3.51 eV to 3.47 and 3.35 eV, respectively. It is predictable that further extensions of the structural modes along the SBz planes

will not decrease the gap significantly. In contrast, as given in Table 2 and Fig. 6, when the number of deckers in the 1D sandwich chains increases from two to six, the HOMO–LUMO gaps decrease from 3.75 to 2.66 eV. We can expect that further addition of new deckers will reduce the gaps continuously, which is important for the generation of conductive or semi-conductive molecular wires. Similarly, as shown in Table 3 and Fig. 6, the

**Table 3** The calculation results, including the point group (PG), lowest vibrational frequencies ( $\nu_{\min}$ , in  $\text{cm}^{-1}$ ), HOMO–LUMO energy gap (Gap, in eV), total binding energies relative to isolated SBz, Bz and Cr ( $\text{BE}_1$ ), average BEs for the formation a HBB ( $\text{BE}_{\text{HBB}}$ ), total BEs relative to the 2D SBz polymers and isolated Bz and Cr ( $\text{BE}_2$ ) and the  $\text{BE}_2$  for extending a decker of the 3D frameworks ( $\text{BE}_{3\text{D-ext}}$ ). All BEs are given in  $\text{kcal mol}^{-1}$

	$\text{BS}^a$	PG	$\nu_{\min}$	Gap	$\text{BE}_1$	$\text{BE}_{\text{HBB}}$	$\text{BE}_2$	$\text{BE}_{3\text{D-ext}}$
<b>2PP<sub>2</sub></b>	BS1	$C_{2v}$	10	3.73	−185.1	−28.7	−151.9	
<b>2PP<sub>3</sub></b>	BS1	$C_{3v}$	13	3.68	−321.1	−28.8	−221.8	
<b>3PP<sub>2</sub></b>	BS1	$D_2$	8	3.56	−330.5	−30.5	−264.0	−102.1 <sup>b</sup>
<b>3PP<sub>3</sub></b>	BS1	$D_{3h}$	11	3.55	−587.3	−30.5	−388.7	−166.9 <sup>b</sup>
<b>2EE<sub>2</sub></b>	BS1	$C_{2v}$	21	3.65	−204.5	−24.0	−147.4	
<b>3EE<sub>2</sub></b>	BS1	$D_{2h}$	21	3.52	−372.1	−25.7	−257.8	−110.4 <sup>b</sup>
<b>2PE<sub>4</sub></b>	BS1	$C_{2v}$	10	3.60	−464.5	−25.3	−286.3	
<b>2PP<sub>2</sub></b>	BS2	$C_{2v}$	11	3.68	−224.8	−29.0	−191.1	
<b>2PP<sub>3</sub></b>	BS2	$C_{3v}$	16	3.64	−380.9	−29.1	−280.5	
<b>2PP<sub>7</sub></b>	BS2	$C_{6v}$	7	3.31	−1032.2	−28.8	−632.2	
<b>3PP<sub>2</sub></b>	BS2	$D_{2h}$	4	3.56	−405.7	−30.9	−338.3	−147.2 <sup>b</sup>
<b>3PP<sub>3</sub></b>	BS2	$D_{3h}$	16	3.53	−700.5	−30.8	−499.6	−219.1 <sup>b</sup>
<b>3PP<sub>7</sub></b>	BS2	$D_{6h}$	19	3.30	−1933.6	−30.4	−1135.6	−503.4 <sup>b</sup>
<b>4PP<sub>2</sub></b>	BS2	$C_2$	9	3.06	−536.2	−29.9	−468.8	−130.5 <sup>c</sup>
<b>4PP<sub>3</sub></b>	BS2	$C_{3v}$	11	3.05	−893.0	−29.7	−692.2	−192.6 <sup>c</sup>
<b>2EE<sub>2</sub></b>	BS2	$C_{2v}$	16	3.62	−243.9	−24.0	−186.5	
<b>2EE<sub>6</sub></b>	BS2	$C_{6v}$	10	3.47	−867.0	−23.3	−532.8	
<b>3EE<sub>2</sub></b>	BS2	$D_{2h}$	21	3.51	−446.5	−25.6	−331.8	−145.3 <sup>b</sup>
<b>3EE<sub>6</sub></b>	BS2	$D_{6h}$	13	3.35	−1625.7	−24.7	−957.2	−424.4 <sup>b</sup>
<b>4EE<sub>2</sub></b>	BS2	$C_{2v}$	13	3.03	−574.0	−24.4	−459.3	−127.5 <sup>c</sup>
<b>2PE<sub>4</sub></b>	BS2	$C_{2v}$	10	3.57	−543.8	−25.3	−364.4	
<b>3PE<sub>4</sub></b>	BS2	$D_{2h}$	18	3.49	−1010.9	−26.9	−652.1	−287.7 <sup>b</sup>
<b>4PE<sub>4</sub></b>	BS2	$C_{2v}$	14	2.98	−1262.1	−25.8	−903.2	−225.8 <sup>c</sup>

<sup>a</sup> BS denotes the basis sets. BS1: 6-311G(d,p), BS2: 6-31G(d). <sup>b</sup> Adding Cr atoms and the SBz polymer ligand decker. <sup>c</sup> Adding Cr atoms and the Bz ligand decker.

HOMO–LUMO gaps will also decrease from the double-decker compounds **2PP<sub>2</sub>** (3.68 eV), **2PP<sub>3</sub>** (3.64 eV), **2EE<sub>2</sub>** (3.62 eV) and **2PE<sub>4</sub>** (3.57 eV) to the quadruple-decker compounds **4PP<sub>2</sub>** (3.06 eV), **4PP<sub>3</sub>** (3.05 eV), **4EE<sub>2</sub>** (3.03 eV) and **4PE<sub>4</sub>** (2.98 eV), respectively, at the B3LYP/BS2 level. Note that adding a Cr–Bz decker will reduce the HOMO–LUMO gaps more than adding a Cr–SBz decker (Fig. 6). The asymmetry in the decreasing ratio of the HOMO–LUMO gaps for extending the structures along different directions suggest that such types of 3D sandwich

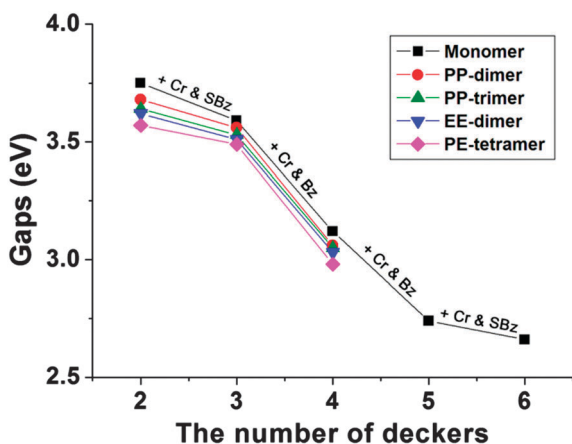


**Fig. 6** The number of deckers of the sandwich compounds vs. HOMO–LUMO gaps (gaps).

frameworks may be useful for designing the directional conductors or semi-conductors.

## 4. Conclusions

Our DFT calculations prove that graphene-like polycyclic aromatic hydrocarbons are not feasible 2D ligands for designing 3D-extensible sandwich compounds (3D-ESC) with uninterrupted sandwich arrays because the  $\pi$ –metal interactions localize the  $\pi$  electrons and then, the ligands cannot maintain their planarity. Thus, we propose that feasible ligands should possess locally delocalized  $\pi$  electrons and we found that our previously reported starbenzene (SBz) polymers match such requirements. SBz polymers can be the feasible ligands of 3D-ESCs because the high degree of  $\pi$  electron delocalization counts little for maintaining its planarity. With the aid of benzene molecules, the SBz polymer can form various mixed-ligand 3D-ESCs. The assembly of 3D-ESCs is largely exothermic, which facilitates their future experimental synthesis. These 3D-ESCs show interesting trends in the variation of their HOMO–LUMO gaps and the 3D-extended sandwich structures may be the directional conductors or semiconductors that are useful in electronic devices.

## Acknowledgements

This study is financially supported by the NSFC (Grant No. 21273140 and 21471092) and the Program for the Outstanding Innovative Teams of Higher Learning Institutions of Shanxi. The authors thank Prof. Zhi-Xiang Wang for constructive discussion.

## Notes and references

- (a) T. J. Kealy and P. L. Pauson, *Nature*, 1951, **168**, 1039; (b) S. A. Miller, J. A. Tebboth and J. F. Tremaine, *J. Chem. Soc.*, 1952, 632; (c) E. O. Fischer and W. Hafner, *Z. Naturforsch., B: Anorg. Chem., Org. Chem., Biochem., Biophys., Biol.*, 1955, **10**, 665.
- For selected recent reviews, see: (a) B. H. Ye and N. Cramer, *Acc. Chem. Res.*, 2015, **48**, 1308; (b) K. Gopalaiah, *Chem. Rev.*, 2013, **113**, 3248; (c) R. G. Arrayas, J. Adrio and J. C. Carretero, *Angew. Chem., Int. Ed.*, 2006, **45**, 7674; (d) V. N. Babin, Y. A. Belousov, V. I. Borisov, V. V. Gumenyuk, Y. S. Nekrasov, L. A. Ostrovskaya, I. K. Sviridova, N. S. Sergeeva, A. A. Simenel and L. V. Snegur, *Russ. Chem. Bull.*, 2015, **63**, 2405; (e) S. S. Braga and A. M. S. Silva, *Organometallics*, 2013, **32**, 5626; (f) E. W. Neuse, *J. Inorg. Organomet. Polym. Mater.*, 2005, **15**, 3; (g) G. S. Kottas, L. I. Clarke, D. Horinek and J. Michl, *Chem. Rev.*, 2005, **105**, 1281; (h) D. R. van Staveren and N. Metzler-Nolte, *Chem. Rev.*, 2004, **104**, 5931.
- (a) N. J. Long, *Metalloenes: An Introduction to Sandwich Complexes*, Blackwell Science, London, 1998; (b) R. H. Crabtree, *The Organometallic Chemistry of the Transition Metals*, Wiley-Interscience, Hoboken, 4th edn, 2005.
- (a) R. N. Grimes, *Pure Appl. Chem.*, 1982, **54**, 43; (b) N. N. Greenwood, *Pure Appl. Chem.*, 1983, **55**, 1415.

- 5 (a) E. Urnezius, W. W. Brennessel, C. J. Cramer, J. E. Ellis and P. v. R. Schleyer, *Science*, 2002, **295**, 832; (b) J. Frunzke, M. Lein and G. Frenking, *Organometallics*, 2002, **21**, 3351.
- 6 (a) S. D. Li, J. C. Guo, C. Q. Miao and G. M. Ren, *Angew. Chem., Int. Ed.*, 2005, **44**, 2158; (b) S. D. Li, C. Q. Miao, G. M. Ren and J. C. Guo, *Eur. J. Inorg. Chem.*, 2006, 2567; (c) S. D. Li, C. Q. Miao and J. C. Guo, *J. Phys. Chem. A*, 2007, **111**, 12069; (d) Q. Luo, X. H. Zhang, K. L. Huang, S. Q. Liu, Z. H. Yu and Q. S. Li, *J. Phys. Chem. A*, 2007, **111**, 2930; (e) L. M. Yang, Y. H. Ding and C. C. Sun, *J. Am. Chem. Soc.*, 2007, **129**, 658; (f) L. M. Yang, Y. H. Ding and C. C. Sun, *J. Am. Chem. Soc.*, 2007, **129**, 1900; (g) L. M. Yang, H. P. He, Y. H. Ding and C. C. Sun, *Organometallics*, 2008, **27**, 1727.
- 7 F. X. Pan, L. J. Li, Y. J. Wang, J. C. Guo, H. J. Zhai, L. Xu and Z. M. Sun, *J. Am. Chem. Soc.*, 2015, **137**, 10954.
- 8 S. Nagao, A. Kato, A. Nakajima and K. Kaya, *J. Am. Chem. Soc.*, 2000, **122**, 4221.
- 9 (a) X. T. Wang, M. Sabat and R. N. Grimes, *J. Am. Chem. Soc.*, 1995, **117**, 12227; (b) X. T. Wang, M. Sabat and R. N. Grimes, *J. Am. Chem. Soc.*, 1994, **116**, 2687.
- 10 (a) V. V. Maslyuk, A. Bagrets, V. Meded, A. Arnold, F. Evers, M. Brandbyge, T. Bredow and I. Mertig, *Phys. Rev. Lett.*, 2006, **97**, 097021; (b) H. J. Xiang, J. L. Yang, J. G. Hou and Q. S. Zhu, *J. Am. Chem. Soc.*, 2006, **128**, 2310; (c) H. X. Da, H. M. Jin, S. W. Yang and K. H. Lim, *J. Phys. Chem. C*, 2009, **113**, 21422; (d) X. J. Wu and X. C. Zeng, *J. Am. Chem. Soc.*, 2009, **131**, 14246; (e) X. Y. Zhang and J. L. Wang, *J. Phys. Chem. A*, 2010, **114**, 2319; (f) Z. H. Zhang, X. J. Wu, W. L. Guo and X. C. Zeng, *J. Am. Chem. Soc.*, 2010, **132**, 10215; (g) J. Jiang, J. R. Smith, Y. Luo, H. Grennberg and H. Ottosson, *J. Phys. Chem. C*, 2011, **115**, 785; (h) Y. C. Li, G. Zhou, J. Wu and W. H. Duan, *J. Chem. Phys.*, 2011, **135**, 014702; (i) X. Y. Zhang, Z. Tian, S. W. Yang and J. L. Wang, *J. Phys. Chem. C*, 2011, **115**, 2948; (j) Y. F. Li, Z. Zhou and Z. F. Chen, *J. Phys. Chem. A*, 2012, **116**, 1648; (k) C. Morari, H. Allmaier, F. Beiușeanu, T. Jurcut and L. Chioncel, *Phys. Rev. B: Condens. Matter Mater. Phys.*, 2012, **85**, 085413; (l) S. C. Zhu, K. L. Yao, G. Y. Gao, W. Yao, Y. Ni and L. Peng, *J. Appl. Phys.*, 2013, **113**, 113901.
- 11 (a) M. R. Philpott and Y. Kawazoe, *Chem. Phys.*, 2007, **337**, 55; (b) M. R. Philpott and Y. Kawazoe, *Chem. Phys.*, 2007, **337**, 223; (c) M. R. Philpott and Y. Kawazoe, *Chem. Phys.*, 2008, **348**, 69.
- 12 M. R. Philpott and Y. Kawazoe, *J. Phys. Chem. A*, 2008, **112**, 2034.
- 13 M. Wu, J. D. Burton, E. Y. Tsymbal, X. C. Zeng and P. Jena, *J. Am. Chem. Soc.*, 2012, **134**, 14423.
- 14 Y. B. Wu, J. L. Jiang, R. W. Zhang and Z. X. Wang, *Chem. – Eur. J.*, 2010, **16**, 1271.
- 15 D. Y. Zubarev and A. I. Boldyrev, *Phys. Chem. Chem. Phys.*, 2008, **10**, 5207.
- 16 M. J. Frisch, G. W. Trucks, H. B. Schlegel, G. E. Scuseria, M. A. Robb, J. R. Cheeseman, G. Scalmani, V. Barone, B. Mennucci, G. A. Petersson, H. Nakatsuji, M. Caricato, X. Li, H. P. Hratchian, A. F. Izmaylov, J. Bloino, G. Zheng, J. L. Sonnenberg, M. Hada, M. Ehara, K. Toyota, R. Fukuda, J. Hasegawa, M. Ishida, T. Nakajima, Y. Honda, O. Kitao, H. Nakai, T. Vreven, J. J. A. Montgomery, J. E. Peralta, F. Ogliaro, M. Bearpark, J. J. Heyd, E. Brothers, K. N. Kudin, V. N. Staroverov, R. Kobayashi, J. Normand, K. Raghavachari, A. Rendell, J. C. Burant, S. S. Iyengar, J. Tomasi, M. Cossi, N. Rega, J. M. Millam, M. Klene, J. E. Knox, J. B. Cross, V. Bakken, C. Adamo, J. Jaramillo, R. Gomperts, R. E. Stratmann, O. Yazyev, A. J. Austin, R. Cammi, C. Pomelli, J. W. Ochterski, R. L. Martin, K. Morokuma, V. G. Zakrzewski, G. A. Voth, P. Salvador, J. J. Dannenberg, S. Dapprich, A. D. Daniels, O. Farkas, J. B. Foresman, J. V. Ortiz, J. Cioslowski and D. J. Fox, *GAUSSIAN 09 (Revision D.01)*, Gaussian, Inc., Wallingford, CT, 2013.
- 17 I. A. Popov, K. V. Bozhenko and A. I. Boldyrev, *Nano Res.*, 2012, **5**, 117.
- 18 (a) R. Hoffmann, R. W. Alder and C. F. Wilcox Jr., *J. Am. Chem. Soc.*, 1970, **92**, 4992; (b) J. B. Collins, J. D. Dill, E. D. Jemmis, Y. Apeloig, P. v. R. Schleyer, R. Seeger and J. A. Pople, *J. Am. Chem. Soc.*, 1976, **98**, 5419; for selected reviews, see: (c) K. Sorger and P. v. R. Schleyer, *THEOCHEM*, 1995, **338**, 317; (d) D. Rottger and G. Erker, *Angew. Chem., Int. Ed. Engl.*, 1997, **36**, 812; (e) L. Radom and D. R. Rasmussen, *Pure Appl. Chem.*, 1998, **70**, 1977; (f) W. Siebert and A. Gunale, *Chem. Soc. Rev.*, 1999, **28**, 367; (g) R. Keese, *Chem. Rev.*, 2006, **106**, 4787; (h) G. Merino, M. A. Mendez-Rojas, A. Vela and T. Heine, *J. Comput. Chem.*, 2007, **28**, 362; (i) L. M. Yang, E. Ganz, Z. F. Chen, Z. X. Wang and P. v. R. Schleyer, *Angew. Chem., Int. Ed.*, 2015, **54**, 9468.
- 19 (a) B. J. Smith, *Chem. Phys. Lett.*, 1993, **207**, 403; (b) W. Tiznado, N. Perez-Peralta, R. Islas, A. Toro-Labbe, J. M. Ugalde and G. Merino, *J. Am. Chem. Soc.*, 2009, **131**, 9426; (c) J. C. Santos, M. Contreras and G. Merino, *Chem. Phys. Lett.*, 2010, **496**, 172; (d) N. Perez-Peralta, M. Contreras, W. Tiznado, J. Stewart, K. J. Donald and G. Merino, *Phys. Chem. Chem. Phys.*, 2011, **13**, 12975; (e) Y. B. Wu, J. L. Jiang, H. G. Lu, Z. X. Wang, N. Perez-Peralta, R. Islas, M. Contreras, G. Merino, J. I. C. Wu and P. v. R. Schleyer, *Chem. – Eur. J.*, 2011, **17**, 714; (f) D. Moreno, G. Martinez-Guajardo, A. Diaz-Celaya, J. M. Mercero, R. de Coss, N. Perez-Peralta and G. Merino, *Chem. – Eur. J.*, 2013, **19**, 12668; (g) J. J. Torres-Vega, A. Vasquez-Espinal, M. J. Beltran, L. Ruiz, R. Islas and W. Tiznado, *Phys. Chem. Chem. Phys.*, 2015, **17**, 19602.